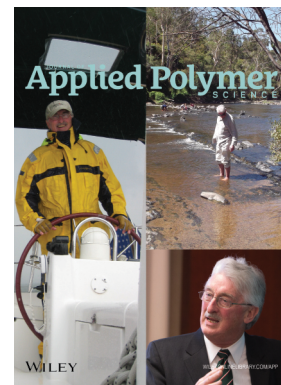


Special Issue: Sustainable Polymers and Polymer Science
Dedicated to the Life and Work of Richard P. Wool

Guest Editors: Dr Joseph F. Stanzione III (Rowan University, U.S.A.)
and Dr John J. La Scala (U.S. Army Research Laboratory, U.S.A.)



EDITORIAL

Sustainable Polymers and Polymer Science: Dedicated to the Life and Work of Richard P. Wool
Joseph F. Stanzione III and John J. La Scala, *J. Appl. Polym. Sci.* 2016, DOI: [10.1002/app.44212](https://doi.org/10.1002/app.44212)

REVIEWS

Richard P. Wool's contributions to sustainable polymers from 2000 to 2015
Alexander W. Bassett, John J. La Scala and Joseph F. Stanzione III, *J. Appl. Polym. Sci.* 2016,
DOI: [10.1002/app.43801](https://doi.org/10.1002/app.43801)

Recent advances in bio-based epoxy resins and bio-based epoxy curing agents
Elyse A. Baroncini, Santosh Kumar Yadav, Giuseppe R. Palmese and Joseph F. Stanzione III, *J. Appl. Polym. Sci.* 2016,
DOI: [10.1002/app.44103](https://doi.org/10.1002/app.44103)

Recent advances in carbon fibers derived from bio-based precursors
Amod A. Ogale, Meng Zhang and Jing Jin, *J. Appl. Polym. Sci.* 2016, DOI: [10.1002/app.43794](https://doi.org/10.1002/app.43794)

RESEARCH ARTICLES

Flexible polyurethane foams formulated with polyols derived from waste carbon dioxide
Mica DeBolt, Alper Kiziltas, Deborah Mielewski, Simon Waddington and Michael J. Nagridge, *J. Appl. Polym. Sci.* 2016,
DOI: [10.1002/app.44086](https://doi.org/10.1002/app.44086)

Sustainable polyacetals from erythritol and bioaromatics
Mayra Rostagno, Erik J. Price, Alexander G. Pemba, Ion Ghiriviga, Khalil A. Abboud and Stephen A. Miller, *J. Appl. Polym. Sci.*
2016, DOI: [10.1002/app.44089](https://doi.org/10.1002/app.44089)

Bio-based plasticizer and thermoset polyesters: A green polymer chemistry approach
Mathew D. Rowe, Ersan Eyiler and Keisha B. Walters, *J. Appl. Polym. Sci.* 2016, DOI: [10.1002/app.43917](https://doi.org/10.1002/app.43917)

The effect of impurities in reactive diluents prepared from lignin model compounds on the properties of vinyl ester resins
Alexander W. Bassett, Daniel P. Rogers, Joshua M. Sadler, John J. La Scala, Richard P. Wool and Joseph F. Stanzione III,
J. Appl. Polym. Sci. 2016, DOI: [10.1002/app.43817](https://doi.org/10.1002/app.43817)

Mechanical behaviour of palm oil-based composite foam and its sandwich structure with flax/epoxy composite
Siew Cheng Teo, Du Ngoc Uy Lan, Pei Leng Teh and Le Quan Ngoc Tran, *J. Appl. Polym. Sci.* 2016, DOI: [10.1002/app.43977](https://doi.org/10.1002/app.43977)

Mechanical properties of composites with chicken feather and glass fibers
Mingjiang Zhan and Richard P. Wool, *J. Appl. Polym. Sci.* 2016, DOI: [10.1002/app.44013](https://doi.org/10.1002/app.44013)

Structure–property relationships of a bio-based reactive diluent in a bio-based epoxy resin
Anthony Maiorana, Liang Yue, Ica Manas-Zloczower and Richard Gross, *J. Appl. Polym. Sci.* 2016, DOI: [10.1002/app.43635](https://doi.org/10.1002/app.43635)

Bio-based hydrophobic epoxy-amine networks derived from renewable terpenoids
Michael D. Garrison and Benjamin G. Harvey, *J. Appl. Polym. Sci.* 2016, DOI: [10.1002/app.43621](https://doi.org/10.1002/app.43621)

Dynamic heterogeneity in epoxy networks for protection applications
Kevin A. Masser, Daniel B. Knorr Jr., Jian H. Yu, Mark D. Hindenlang and Joseph L. Lenhart, *J. Appl. Polym. Sci.* 2016,
DOI: [10.1002/app.43566](https://doi.org/10.1002/app.43566)

Special Issue: Sustainable Polymers and Polymer Science
Dedicated to the Life and Work of Richard P. Wool

Guest Editors: Dr Joseph F. Stanzione III (Rowan University, U.S.A.)
and Dr John J. La Scala (U.S. Army Research Laboratory, U.S.A.)

Statistical analysis of the effects of carbonization parameters on the structure of carbonized electrospun organosolv lignin fibers

Vida Poursorkhabi, Amar K. Mohanty and Manjusri Misra, *J. Appl. Polym. Sci.* 2016, DOI: 10.1002/app.44005

Effect of temperature and concentration of acetylated-lignin solutions on dry-spinning of carbon fiber precursors

Meng Zhang and Amod A. Ogale, *J. Appl. Polym. Sci.* 2016, DOI: 10.1002/app.43663

Poly(lactic acid) bioconjugated with glutathione: Thermosensitive self-healed networks

Dalila Djidi, Nathalie Mignard and Mohamed Taha, *J. Appl. Polym. Sci.* 2016, DOI: 10.1002/app.43436

Sustainable biobased blends from the reactive extrusion of polylactide and acrylonitrile butadiene styrene

Ryan Vadori, Manjusri Misra and Amar K. Mohanty, *J. Appl. Polym. Sci.* 2016, DOI: 10.1002/app.43771

Physical aging and mechanical performance of poly(L-lactide)/ZnO nanocomposites

Erlantz Lizundia, Leyre Pérez-Álvarez, Míriam Sáenz-Pérez, David Patrocínio, José Luis Vilas and Luis Manuel León, *J. Appl. Polym. Sci.* 2016, DOI: 10.1002/app.43619

High surface area carbon black (BP-2000) as a reinforcing agent for poly[(-)-lactide]

Paula A. Delgado, Jacob P. Brutman, Kristina Masica, Joseph Molde, Brandon Wood and Marc A. Hillmyer, *J. Appl. Polym. Sci.* 2016, DOI: 10.1002/app.43926

Encapsulation of hydrophobic or hydrophilic iron oxide nanoparticles into poly-(lactic acid) micro/nanoparticles via adaptable emulsion setup

Anna Song, Shaowen Ji, Joung Sook Hong, Yi Ji, Ankush A. Gokhale and Ilsoon Lee, *J. Appl. Polym. Sci.* 2016, DOI: 10.1002/app.43749

Biorenewable blends of polyamide-4,10 and polyamide-6,10

Christopher S. Moran, Agathe Barthelon, Andrew Pearsall, Vikas Mittal and John R. Dorgan, *J. Appl. Polym. Sci.* 2016, DOI: 10.1002/app.43626

Improvement of the mechanical behavior of bioplastic poly(lactic acid)/polyamide blends by reactive compatibilization

JeongIn Gug and Margaret J. Sobkowicz, *J. Appl. Polym. Sci.* 2016, DOI: 10.1002/app.43350

Effect of ultrafine talc on crystallization and end-use properties of poly(3-hydroxybutyrate-co-3-hydroxyhexanoate)

Jens Vandewijngaarden, Marius Murariu, Philippe Dubois, Robert Carleer, Jan Yperman, Jan D'Haen, Roos Peeters and Mieke Buntinx, *J. Appl. Polym. Sci.* 2016, DOI: 10.1002/app.43808

Microfibrillated cellulose reinforced non-edible starch-based thermoset biocomposites

Namrata V. Patil and Anil N. Netravali, *J. Appl. Polym. Sci.* 2016, DOI: 10.1002/app.43803

Semi-IPN of biopolyurethane, benzyl starch, and cellulose nanofibers: Structure, thermal and mechanical properties

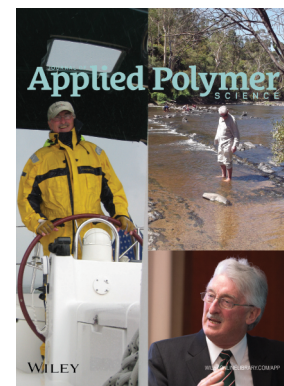
Md Minhaz-Ul Haque and Kristiina Oksman, *J. Appl. Polym. Sci.* 2016, DOI: 10.1002/app.43726

Lignin as a green primary antioxidant for polypropylene

Renan Gadioli, Walter Ruggeri Waldman and Marco Aurelio De Paoli *J. Appl. Polym. Sci.* 2016, DOI: 10.1002/app.43558

Evaluation of the emulsion copolymerization of vinyl pivalate and methacrylated methyl oleate

Alan Thyago Jensen, Ana Carolina Couto de Oliveira, Sílvia Belém Gonçalves, Rossano Gambetta and Fabricio Machado *J. Appl. Polym. Sci.* 2016, DOI: 10.1002/app.44129



Microfibrillated cellulose-reinforced nonedible starch-based thermoset biocomposites

Namrata V. Patil, Anil N. Netravali

Department of Fiber Science & Apparel Design, Cornell University, Ithaca, New York 14853

Correspondence to: A. Netravali (E-mail: ann2@cornell.edu)

ABSTRACT: The present research focuses on developing nonedible starch-based resin to replace the currently used edible starches (corn, potato, etc.), protein (soy) as well as some of the petroleum-based resins for fiber-reinforced composite applications. Starch was extracted from mango seeds, a waste source freely available in tropical countries. Micro fibrillated cellulose (MFC) obtained from kraft pulp was used to reinforce mango seed starch-based resin in order to take advantage of the chemical similarity between the starch and the cellulose which results in good interfacial bonding. Uniform dispersion of MFC in starch was obtained using homogenizer. Further, this MFC/MSS mixture was crosslinked using an environment friendly crosslinker, 1,2,3,4-butane tetracarboxylic acid (BTCA). Crosslinking was confirmed directly using ATR-FTIR spectra. MFC/MSS biocomposite specimens were prepared by solution casting method. The characterization of MFC/MSS biocomposites showed that their tensile and thermal properties were comparable to the edible starch-based composites. The thermoset resins obtained from agricultural mango seed waste can be used to replace currently available resins derived from the edible sources or even some petroleum-based resins for packaging, coatings, mulches, and other applications. © 2016 Wiley Periodicals, Inc. *J. Appl. Polym. Sci.* **2016**, *133*, 43803.

KEYWORDS: biodegradable; composites; crosslinking; mechanical properties; thermosets

Received 21 February 2016; accepted 18 April 2016

DOI: 10.1002/app.43803

INTRODUCTION

Synthetic polymers are widely used in a broad range of applications from agriculture (e.g., Mulch films) to furniture and from casing and packaging for consumer products (e.g., flexible plastic bags or rigid containers) to fiber reinforced composites for aerospace and automobiles because of their low density and excellent mechanical properties. Some of their other properties such as high molecular weight and chemical stability, while critical during their use, makes it difficult for them to be degraded by microbes and they persist in nature for long time after disposal.^{1,2} Another major problem associated with the synthetic polymers is that the monomers used to synthesize them are petroleum-based, a nonsustainable commodity. The depleting petroleum stock and increasing problems related to their end-of-life disposal calls for bio-based materials to substitute these nonbiodegradable petroleum-based polymers.³ Accordingly, numerous researchers have been developing materials using plant-based and sustainable polymer sources such as starch, protein, lignin, cellulose, etc.^{4–10} Starch from corn, rice, wheat, potato and many others have received special attention for making environment-friendly materials during the past few decades

as they are inexpensive, biodegradable and available worldwide.¹¹ Corn and other edible starches, for example, are being used extensively on an industrial scale for production of bio-fuels, chemicals and plastics.^{10,12} However, the use of such edible starches for nonfood applications have raised ethical questions as they contain nutritional values for humans as well as livestock diet. Although starches are derived from yearly renewable sources, the increase in world population and food shortage around the world will restrict the use of edible resources for industrial scale applications in the future.¹³ On the other hand, the residues (defatted seed cakes) from many agro-seeds from which oils/fats are extracted for use in food or cosmetics remain mostly as waste. These defatted seed cakes are rich sources of secondary metabolites consisting mostly of starch and/or protein which can be easily extracted and used for nonfood applications as bio-based green resins for fiber reinforced composites or films for packaging, coatings, mulches, etc.^{14,15}

Magnifera Indica, commonly known as mango is cultivated on a large scale in tropical countries.¹⁶ The mango fruit is not only eaten but ripe mangoes are also processed on a large scale for conversion to juices, jams, fruit cheeses, ice-creams and variety of other products. After processing of mangoes on an industrial

Additional Supporting Information may be found in the online version of this article.

© 2016 Wiley Periodicals, Inc.

gelatinize it. Gelatinization of MSS is important as it ruptures the granular starch wall allowing the hydroxyl groups present on the starch to be accessible for crosslinking reaction. After gelatinization, predetermined amount of crosslinker, BTCA, (based on the stoichiometry) and catalyst, NaP (50 wt% of BTCA),^{26,27} were added to the gelatinized starch solution and allowed to react for an additional 1 h at 90 °C with constant stirring at 200 rpm to ensure complete dissolution and mixing of BTCA and NaP and formation of viscous homogeneous MSS solution. This solution was then poured onto a Teflon[®] coated glass plate (100 mm × 100 mm) and allowed to dry at room temperature until the film could be peeled off the plate easily. It was then cured (crosslinked) using Carver Hydraulic hot-press (model 3891-4PROA00, Wabash, IN) at 140 °C for 15 min under a pressure of 0.38 MPa. This crosslinking process is a slight modification of the process used earlier to crosslink edible corn and potato starch.^{5,27} The crosslinked films were then washed using DI water to remove the excess unreacted BTCA and NaP as they are hygroscopic and tend to absorb moisture. The films were conditioned at the ASTM conditions of 21 °C ± 1 °C and 65% ± 1% RH for 48 h before testing.

Preparation of Crosslinked MFC/MSS Biocomposites

MFC was used to reinforce MSS and further crosslinked to obtain high strength MFC/MSS biocomposites. 4 g of MSS and MFC together, containing varying ratios of MFC:MSS (20:80, 30:70 and 40:60) were mixed in 150 mL of water and dispersed well using a VWR[®] 250 homogenizer equipped with VWR[®] 20 × 115 mm saw-tooth generator probe at 20,000 rpm for 10 min and then stirred overnight at 1000 rpm using a magnetic stirrer. This dispersion was then heated at 90 °C for 1 h in order to gelatinize MSS with constant stirring at 1000 rpm to prevent the clustering of MFC fibrils. Predetermined amount of BTCA and NaP were added to this gelatinized solution and further heated at 90 °C while continued stirring at 1000 rpm. This is termed as pre-cured mixture which was poured onto a Teflon[®]-coated glass plate and dried. The dried sheets were cured at 140 °C to complete the crosslinking reaction. The crosslinked sheets were then washed and conditioned following the same procedure described above.

Preparation of Crosslinked MFC Films

Pure MFC films were made in order to study the crosslinking of MFC using BTCA as a crosslinker and NaP as a catalyst. 4 g of MFC was dispersed uniformly in 150 mL of DI water using the VWR[®] 250 homogenizer equipped with VWR[®] 20 × 115 mm saw-tooth generator probe at 20,000 rpm for 10 min and then stirred overnight at 1000 rpm using a magnetic stirrer. BTCA, 40% by wt. was added to the dispersed MFC. NaP (50% by wt of BTCA) was added as a catalyst for possible esterification reaction between the carboxylic groups of BTCA and hydroxyl groups of MFC. This mixture was pre-cured at 90 °C with constant magnetic stirring at 1000 rpm for 1 h after which it was poured onto the Teflon[®]-coated glass plate and dried, cured, washed, and conditioned following the same procedure described above.

Proximate Chemical Composition Analysis

Proximate chemical analysis of the as received DMSC and the extracted MSS was performed to determine the chemical composition of both. Moisture, starch, water and ethanol soluble carbohydrate, crude protein, crude fiber, crude fat and ash contents were determined using Association of Analytical Communities (AOAC) standards. To analyze starch content, samples were pre-extracted for sugar by incubation in a water bath at 40 °C and filtered using a Whatman[®] 41 filter paper. The residue was thermally solubilized using an autoclave and incubated with glucoamylase enzyme to hydrolyze starch to produce dextrose (glucose). These samples were then injected into sample chamber of YSI 2700 SELECT Biochemistry Analyzer (Yellow Springs, Ohio) where it was allowed to diffuse into a membrane containing glucose oxidase. The dextrose was immediately oxidized to hydrogen peroxide and D-glucono-4-lactone. Hydrogen peroxide (H₂O₂) was detected amperometrically at the platinum electrode surface. The current flow at the electrode is directly proportional to the H₂O₂ concentration and hence to dextrose concentration. Starch amount was determined by multiplying dextrose by 0.9. All analysis was performed at Dairy One, Ithaca, NY, in triplets to ensure the reproducibility of the results.

ATR-FTIR Analysis

ATR-FTIR spectra of BTCA, MFC and crosslinked MSS, MFC, and MFC/MSS biocomposites were obtained to confirm the crosslinking reaction of MSS and MFC with BTCA as a crosslinker and NaP as a catalyst. Pure MSS and MFC were crosslinked, separately, using BTCA and NaP to confirm if BTCA can esterify MSS and MFC, individually. The ATR-FTIR spectra were collected using Thermo Nicolet Magna-IR 560 spectrometer (Madison, WI) with a split pea accessory. Each scan was an average of 150 scans from 4000 cm⁻¹ to 500 cm⁻¹ wavenumbers.

Scanning Electron Microscopy

Granular structure of MSS before and during the gelatinization process and the fracture surfaces of the MFC-MSS biocomposites fractured during tensile testing were studied using LEO 1550 field emission scanning electron microscope (Germany). The specimens were placed on standard aluminum specimen mounts with double sided electrically conductive carbon tape (SPI supplies, West Chester, PA). In order to avoid charging, specimens were carbon coated in a vacuum coater (model BTT IV, Denton Vacuum, Moorestown, NJ). The coated specimens were observed on the SEM using accelerating voltage of 1 kV to study the MSS granular structure and using accelerating voltage of 2 kV to study the fracture surfaces of composites and surface topographies with protruding fibers.

Characterization of Tensile Properties

The prepared biocomposites were characterized for their tensile properties to study the effect of addition of MFC to MSS as well as crosslinking. Specimens of 50 mm × 10 mm dimensions were cut randomly from different parts of the conditioned crosslinked MSS films as well as MFC/MSS biocomposite films. Tensile properties were characterized using Instron Universal Tester (Instron), model 5566 (Instron Co., Canton, MA), according to ASTM D882-02 standard and properties including fracture stress (tensile strength), fracture strain and Young's

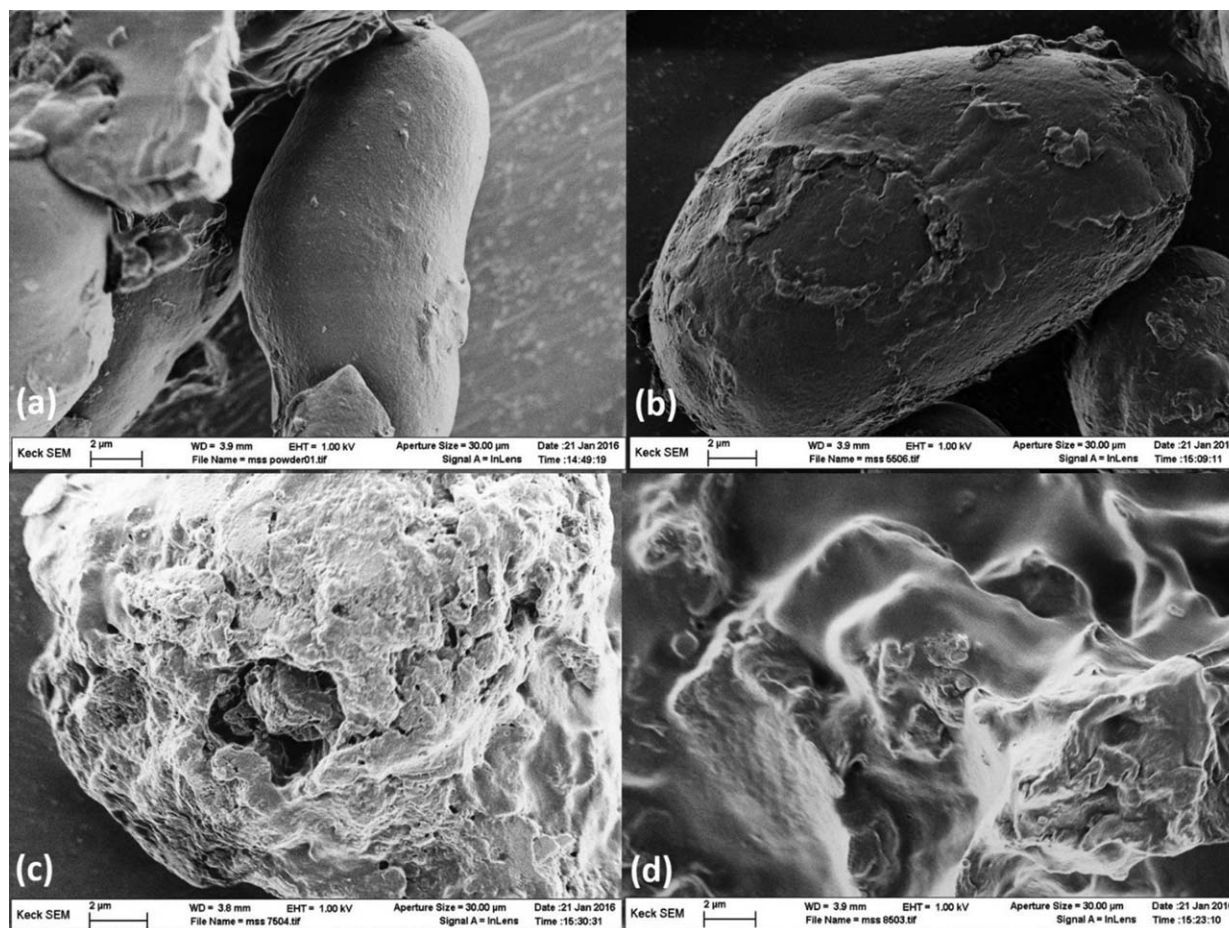


Figure 1. SEM images of MSS granules (a) at room temperature and MSS solution heated in water with constant stirring at (b) 65°C, (c) 75°C, (d) 85°C.

modulus were determined. The film thickness was measured using a vernier caliper at three different locations along the length of each conditioned specimen and the average of the three readings was used to calculate the specific tensile properties. Roughly, the thickness was found to be $0.2 \text{ mm} \pm 0.1 \text{ mm}$. The specimen gauge length was adjusted to 30 mm and the strain rate was 0.6 min^{-1} . Specimens were tested from three different films of each type cast at different times, to ensure reproducibility of the results. At least three specimens from each of the films produced at three different times were used for calculating average and standard deviation values.

Characterization of Thermal Properties

Thermogravimetric analysis (TGA) of MSS, crosslinked MSS and crosslinked MFC/MSS biocomposites was performed to characterize their thermal stability and degradation characteristics. TGA-2050, TA Instruments, Inc. (New Castle, DE) was used for these tests. Specimens weighing 5 to 10 mg were scanned from 25°C to 600°C on the TGA at a heating ramp rate of 10°C/min in a nitrogen gas flow of 60 mL/min.

RESULTS AND DISCUSSION

Proximate Chemical Composition Analysis

Proximate chemical composition analysis revealed that DMSC was rich in starch. It consisted of 43% starch, 11.5% moisture, 12.6%

protein, 13% of water-soluble sugars, and 5.2% of ethanol-soluble sugars. It also had traces of crude fat, fiber and ash. MSS, after the extraction process, consisted of 60% starch, 3% moisture, 13% protein, 6.3% of water-soluble sugars, and 0.4% of ethanol-soluble sugars. It is clear that the simple and water-based filtration process used for MSS extraction resulted in a significant increase in the starch content as it removed significant amount of water soluble sugars and other components from the DMSC. Higher amount of starch is desirable for making the resin as the tensile properties of the resin depend on the higher molecular weight of the starch. The properties can be increased further by crosslinking.^{5,27} In addition, as discussed later, by adding MFC, even higher tensile properties can be obtained.²⁷ MSS was also washed with ethanol instead of water using the same procedure with an idea to further remove simple sugars. However, the starch content in the extracted MSS was not found to increase significantly. As a result, only water washing was used to extract starch to keep the process “green” and free from any solvents.

Granule Morphology and Gelatinization Behavior of MSS

The granular morphology and the gelatinization behavior of the extracted MSS was studied using SEM. Figure 1 shows the SEM images of MSS granules at room temperature and MSS solution heated in a water bath with constant stirring at 65°C, 75°C, and 85°C. As seen in Figure 1(a), MSS granules were found to

be oval in shape and the average granule size was found to be in the range of 8 to 12 μm in width and 20 to 25 μm in length. Similar shape and granule size distribution were found by Kaur *et al.*¹⁶ who studied the morphology of starch extracted from seeds of five different varieties of mangoes. Starches such as potato and corn have round to oval and irregular shaped granules, respectively, with their size ranging from 8 to 30 μm .^{28,29} Starch, a mixture of branched amylopectin and linear amylose, is semi crystalline in nature.¹¹ The branches of amylopectin molecules form double helices which are arranged in crystalline domains and accounts for the crystallinity of starch while the amylose molecules are associated with the amorphous regions.¹¹ Figure 1(b) shows MSS granule heated in water at 65 °C. The granule is clearly seen to be swollen many folds because of the absorbed water in the amorphous region as a result of weak hydrogen bonding.²⁸ It is known that when further heated to higher temperatures, the swelling continues, and the granular structure of starch collapses with the loss in crystalline order.²⁸ This is very well illustrated in Figures 1(c,d). As seen in Figure 1(c), at 75 °C, the granules of starch are swollen so much that they have ruptured. The rupturing of granule boundary leads to uncoiling and dissociation of double helices and both amylose and amylopectin leach out from inside the granule forming homogenous and viscous starch solution.²⁹ This viscous solution is seen in Figure 1(d). At this point, the hydroxyl groups from amylose and amylopectin are readily accessible for any reaction. The swelling and rupturing of starch granules is commonly known as gelatinization and different starches show different gelatinization temperatures due to their different amylose and amylopectin content based on their biological origins. For example, potato and corn starches have gelatinization temperatures of 65 °C and 70 °C, respectively.^{30,31} Based on the understanding derived from Figure 1, it can be concluded that MSS was completely gelatinized at 85 °C. Further, the gelatinization temperature of MSS was confirmed using Advance Rheometer-2000 (TA Instruments, New Castle, DE) equipped with standard steel parallel plate and found to be 80 °C.²⁶

Attenuated Total Reflectance-Fourier Transform Infrared (ATR-FTIR) Analysis

ATR-FTIR analysis was performed to confirm the crosslinking of starch and cellulose using BTCA. Figure 2 shows ATR-FTIR spectra of BTCA, MSS, crosslinked MSS, MFC, crosslinked MFC and crosslinked MFC/MSS biocomposite. A sharp peak was observed in BTCA spectrum at 1689 cm^{-1} corresponding to carbonyl in the carboxylic acid groups. MSS showed peaks in the finger print region as observed in other pure starches such as corn or potato and no peaks were seen in the carbonyl region as can be expected.⁵ However, crosslinked MSS showed a peak at 1720 cm^{-1} corresponding to the carbonyl from ester groups. This confirmed the esterification reaction between the carboxyl groups from BTCA and the hydroxyl groups from MSS which takes place during the curing (hot-pressing). The BTCA crosslinks with MSS via anhydride formation (Scheme 1) in the presence of the catalyst (NaP) which, in turn, reacts with the hydroxyl groups abundantly present and easily available due to gelatinization of MSS.²⁶ BTCA and NaP have been used to crosslink cellulose earlier.³² Thus, BTCA can be used to cross-

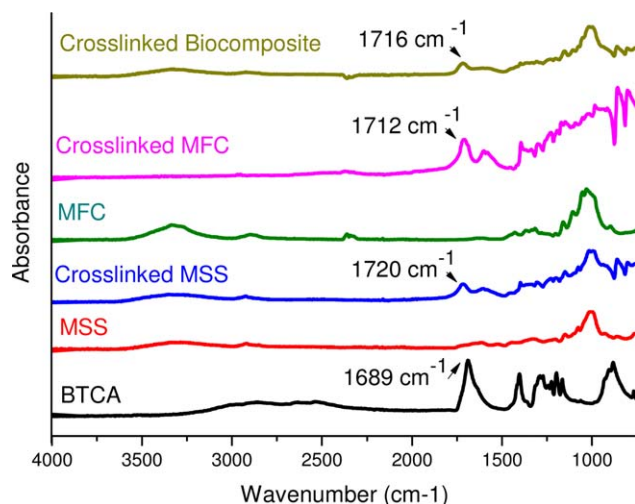


Figure 2. ATR-FTIR spectra of BTCA, MSS, crosslinked MSS, MFC, crosslinked MFC and crosslinked MFC/MSS biocomposite. [Color figure can be viewed in the online issue, which is available at wileyonlinelibrary.com.]

link MFC as well because of the hydroxyl groups present on MFC. To confirm the crosslinking of cellulose with BTCA, pure MFC was reacted with BTCA according to the procedure mentioned above and the ester peak was observed at 1712 cm^{-1} due to the crosslinking which occurs while curing. It should be noted that a minimum temperature of 140 °C is required to crosslink MFC as no ester peak was observed in ATR-FTIR spectrum when the curing was carried out below 140 °C. While temperatures higher than 140 °C will be beneficial for crosslinking MFC, the MFC/MSS biocomposite was not cured above 140 °C to avoid any degradation of MSS. The crosslinked MFC/MSS biocomposite films consisting of MSS and MFC also showed the ester peak at 1716 cm^{-1} confirming the formation of a crosslinked biocomposite.

TENSILE PROPERTIES

Effect of Crosslinker Ratio on MSS

Figure 3(a) shows the effect of BTCA concentration on tensile strength and Young's modulus of the crosslinked MSS films. It was observed that both tensile strength and Young's modulus values increased from 3.5 to 16 MPa and from 300 MPa to 1.3 GPa, respectively, after crosslinking. The increase in both tensile strength and modulus values with increased BTCA concentration, seen in Figure 3(a) was due to covalent bond formation (crosslinking) which interconnects starch molecules in the film and thereby increases the molecular weight of MSS as well as the rigidity of the system.³³ However, the results also indicated that an optimum amount of BTCA was necessary to obtain desired increase in tensile strength and Young's modulus. Concentrations below 40% provided increase in the tensile strength and modulus while concentration above 40% showed reduction in tensile strength and modulus. Highest tensile strength and modulus was observed when BTCA concentration was 40%. This agrees well with the stoichiometric calculation which suggests 37.5% BTCA is required for complete crosslinking of starch. When the concentration of BTCA increased to 45%, there was a decrease in both tensile strength and modulus.

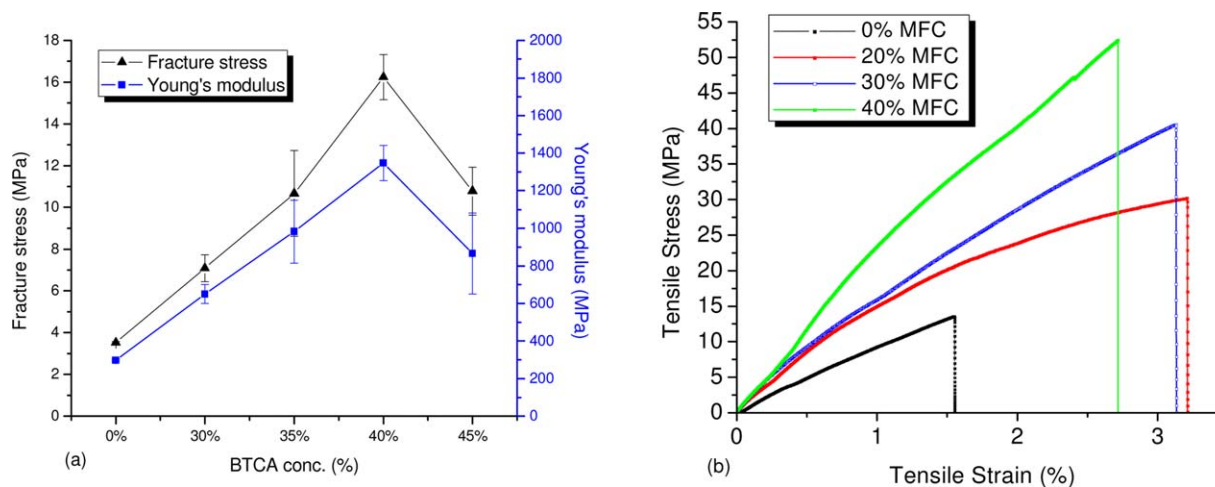


Figure 3. (a) Effect of BTCA concentration on tensile (fracture) stress and Young's modulus of the crosslinked MSS films (b) Representative stress-strain curve of crosslinked MFC/MSS biocomposite with different MFC loadings. [Color figure can be viewed in the online issue, which is available at wileyonlinelibrary.com.]

The decrease in strength and modulus might be due to the presence of unreacted or partially reacted carboxylic groups in the excess BTCA which did not come out in washing. These unreacted COOH groups have been shown to absorb moisture during conditioning and plasticize the films, reducing their tensile properties.³³ The tensile strength and modulus of cross-linked MSS using 40% BTCA was found to be 16 MPa and 1.3 GPa, respectively, which is comparable to the resins prepared from commercially available waxy maize starch.²⁷ The tensile strength and modulus of the crosslinked waxy maize starch was reported to be 17 MPa and 1.3 GPa, respectively.²⁷ Thus, MSS obtained from waste mango seed biomass can be easily used to replace commercially available edible starches for nonedible applications. The Young's modulus of neat synthetic polymers such as polypropylene (PP) and polyethylene (PE) have been reported to be 1.4 and 0.4 GPa, respectively.^{34,35} Thus, cross-linked MSS resin can not only replace edible starch-based polymers but also some petroleum-based plastics such as PP or PE.

Effect of MFC Loading

MFC was used to reinforce MSS resin and the effect of MFC loading was studied. Figure 3(b) shows representative stress-strain curves of crosslinked MFC/MSS biocomposite films with different MFC loadings and Table I presents the tensile properties of the crosslinked MFC/MSS biocomposite films for different MFC loadings. A significant increase in the tensile strength and modulus was observed with the addition of MFC to the MSS resin. This is not only because of the excellent tensile

properties of MFC but also because it has a very high aspect ratio and provides high surface area for bonding with MSS. In addition, the chemical similarity between cellulose and starch provide ample opportunity for crosslinking as well as hydrogen bonding which leads to strong adhesion between MFC and MSS. Chemical similarity also allows excellent wetting of MFC by water-based MSS resin. The proposed crosslinking reaction shown in Scheme 1 was confirmed using ATR-FTIR spectra shown in Figure 2. Excellent fiber/resin bonding was also confirmed from the SEM images of fracture surfaces (Figure 4, discussed in the next section) which showed no protruding MFC fibrils for crosslinked MSS containing MFC. Excellent fiber/resin bonding contributes to an effective load transfer from broken to unbroken fibrils and, thus, results in higher strength and the Young's modulus of the composites.³⁶ As seen from data presented in Table I, the fracture strain of the MFC/MSS biocomposites increased from 1.65% for control (without MFC) to about 3.9% as the MFC content was increased to 20% or 30%. This is thought to be because of the crack bridging mechanism provided by the MFC. However, at 40% MFC, with slight clustering of fibrils, the fracture strain decreased to 2.65%. Moisture content, however, decreased steadily with increase in the MFC content (Table I). This was due to the fact that MFC is highly crystalline and does not provide space for the moisture to enter. As a result, it can act as a barrier for moisture, providing a significant advantage to obtain desirable mechanical properties. Uniform dispersion of MFC is, however, the key to improving the strength and the modulus of the composites. Almost 24%

Table I. Tensile Properties of Crosslinked MFC/MSS Biocomposites with Different MFC Loadings

MFC:MSS Biocomposites	Fracture stress (MPa)	Fracture strain (%)	Young's modulus (MPa)	Moisture content (%)
0:100	16.24 (1.98)	1.54 (0.56)	1347 (324)	8.8
20:80	31.17 (7.01)	3.80 (0.72)	1667 (275)	7.3
30:70	38.69 (3.00)	3.95 (0.77)	1780 (221)	6.0
40:60	50.03 (1.97)	2.65 (0.13)	2407 (063)	5.8

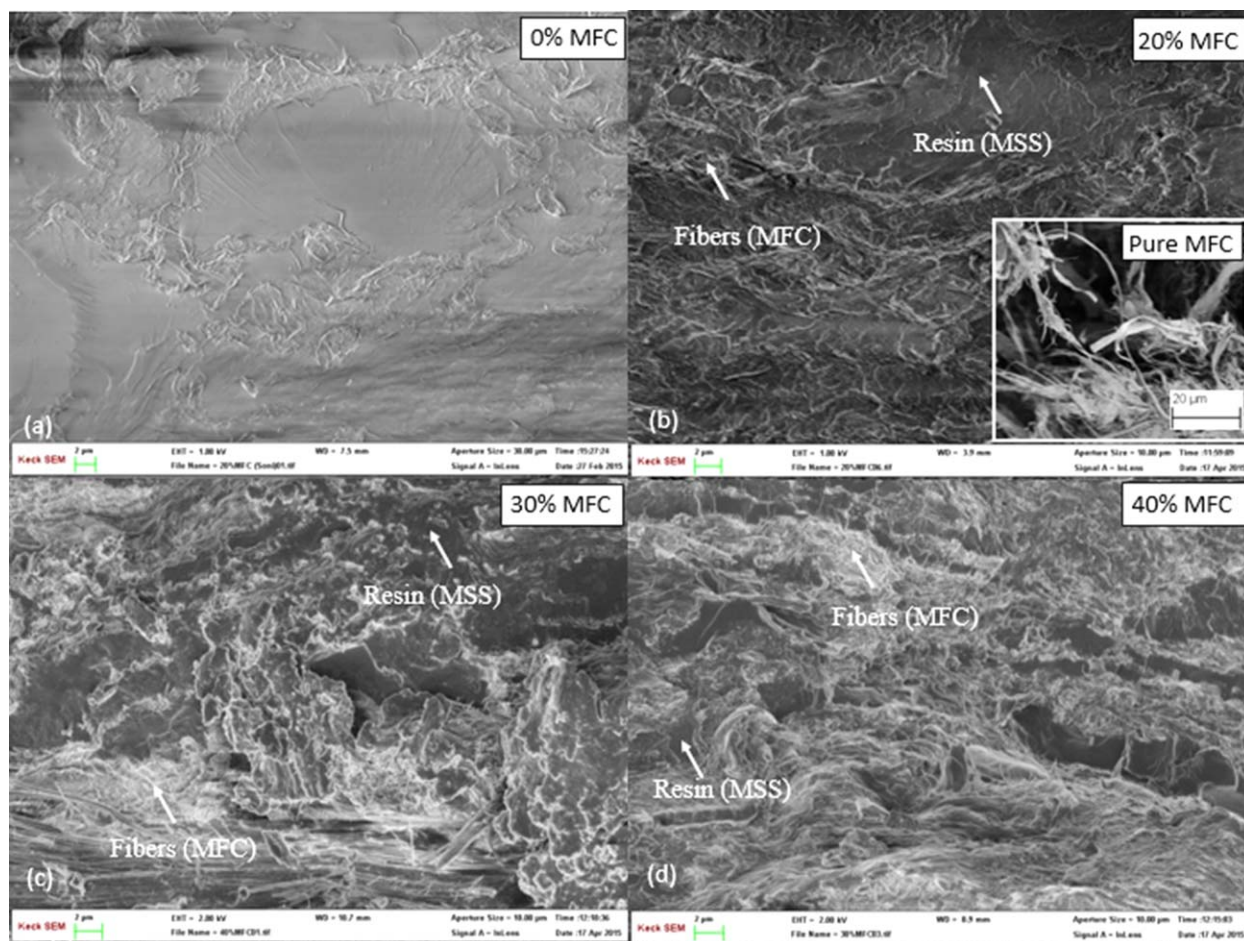


Figure 4. SEM images of fracture surfaces of crosslinked MFC/MSS biocomposites with different MFC loadings, fractured during tensile testing. Inset in (b) shows SEM image of pure MFC. [Color figure can be viewed in the online issue, which is available at wileyonlinelibrary.com.]

increase in the modulus was obtained by adding 20% MFC to the MSS resin while it increased by 32% with 30% MFC addition. Significant improvement in the properties was obtained by adding 40% MFC which resulted in almost 79% increase in Young's modulus. Similar behavior was observed by Ghosh Dastidar and Netravali²⁷ when MFC was added to waxy maize starch. They reported that MFC can act as crack-bridging mechanism and could be a potential substitute to commonly used plasticizers like glycerol or sorbitol for toughening, while also strengthening the resin. Stress vs. strain curves in Figure 3(b) confirm that MFC addition increases the toughness of the MSS resin. The tensile properties of crosslinked MFC/MSS biocomposites were found to be comparable to MFC/Soy protein concentrate biocomposites, MFC/waxy maize biocomposites, MFC/PVA as well as MFC/PPbased composites.^{27,37–39}

Scanning Electron Microscopy

Scanning Electron Microscopy (SEM) was used to study the fractured surfaces of the MFC/MSS biocomposites. Figure 4 shows the fracture surfaces of crosslinked MFC/MSS biocomposite specimens with different MFC loadings, fractured during the tensile testing. Figure 4(a) shows the fracture surface of pure MSS crosslinked resin without any MFC. The fracture surface topography of

crosslinked resin was smooth as there were no fibers. Figure 4(b–d) show the fracture surfaces of the crosslinked MFC/MSS biocomposites with 20%, 30% and 40% MFC loadings, respectively. Please note that Figure 4(b) inset shows an SEM image of pure MFC. The fracture surfaces of MFC/MSS biocomposites were rough compared to pure MSS crosslinked resin due to the presence of the fibrils and the roughness increased with the increase in MFC content. The SEM images of the crosslinked MFC/MSS biocomposites in Figure 4(b–d) also show that MFC was well embedded into the MSS resin due to crosslinking as opposed to those in Supporting Information Figure S1 which show MFC fibers agglomerated in bundles and protruding out from the resin for noncrosslinked MFC/MSS biocomposite specimens. As stated earlier, the crosslinking of MSS and MFC which was confirmed directly using ATR-FTIR spectra shown earlier in Figure 2 leads to the formation of covalent bonds which are much stronger than the hydrogen bonds, earlier present between MFC and MSS. In order to achieve good mechanical properties for MFC/MSS biocomposites, good dispersion of fibrils within the resin, effective wetting of fibers by resin and good interfacial bonding is required.⁴⁰ Homogenization of MSS and MFC together helped to obtain better dispersion of MFC in MSS and crosslinking them increased the covalent bonding between MFC and MSS.

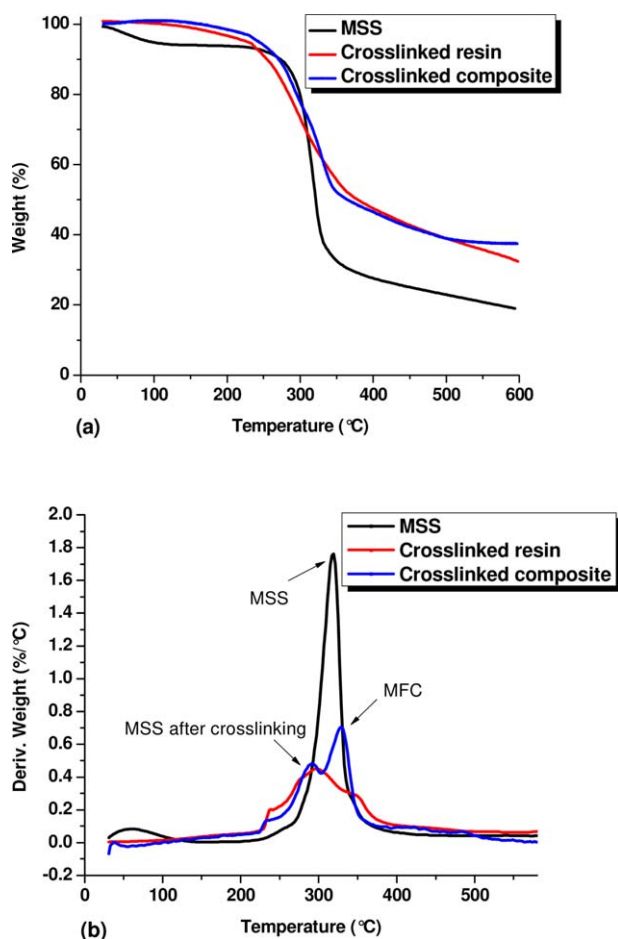


Figure 5. (a) TGA thermograms of MSS, crosslinked resin and crosslinked MFC/MSS biocomposites (b) DTGA thermograms of MSS, crosslinked MSS resin and crosslinked MFC/MSS biocomposites. [Color figure can be viewed in the online issue, which is available at wileyonlinelibrary.com.]

Thermal Properties

The thermal stability of the MFC/MSS biocomposites was examined using TGA. Figure 5(a) shows typical TGA thermograms of MSS, crosslinked MSS resin, and the crosslinked MFC/MSS biocomposite. DTGA thermograms, constructed from the TGA thermograms of MSS, crosslinked MSS resin and the crosslinked MFC/MSS biocomposites are presented in Figure 5(b). As can be seen in Figure 5(a), the onset degradation temperature (T_d) was same (220 °C) for the crosslinked MSS resin as well as the crosslinked MFC/MSS biocomposite, both of which, however, were slightly lower than MSS (250 °C). This is due to the presence of some unreacted carboxylic groups of BTCA.⁴¹ Similar results were obtained by Zhang *et al.* who treated corn starch with oxalic acid.⁴¹ It was observed that the weight loss reduced after crosslinking MSS and further on addition of MFC. For example, at 600 °C, 80% weight loss was observed for pure MSS (control). However, crosslinked MSS resin and crosslinked MFC/MSS biocomposite specimens showed weight loss of only 60% at 600 °C. As seen in Figure 5(b), the DTGA plot for pure MSS showed a maximum degradation peak at 315 °C while the crosslinked MSS showed the peak at 295 °C. Also, both crosslinked resin and the MFC/MSS

biocomposite showed gradual degradation as compared to that of MSS. The DTGA of crosslinked MFC/MSS biocomposite showed a two stage degradation with the first degradation beginning at 295 °C which was same as that observed for the crosslinked MSS. The second stage of degradation was observed at 340 °C which corresponds to the degradation of MFC. The TGA analysis indicates that the addition of MFC does not alter the thermal stability of the composite, particularly the resin part. This is because both MSS and MFC exist as separate phases and do not affect each other.⁴² This is in contrast to other reinforcing agents such as nanoclay, which are inorganic and being thermally very stable lead to an increased thermal stability of the composites. Also, the nanoclay has dimensions in the nanometer range whereas most of MFC exists in the micrometer range.

CONCLUSIONS

This paper showed the possibility of utilizing freely available by-products from food industries or agricultural residues such as mango seed cake rather than edible starches for applications in biobased resins and composites. A biodegradable starch-based resin was obtained using MSS and crosslinked using a benign crosslinker/catalyst (BTCA/NaP) combination to obtain desirable tensile properties. The results indicated that 40% concentration of BTCA results in highest tensile strength and Young's modulus of the MSS resin. The effect of MFC loading on MSS and crosslinked MSS properties was also studied. Significant improvements in the tensile properties of MSS were observed after incorporating MFC. MFC/MSS biocomposites with tensile strength of 50 MPa and Young's modulus 2.4 GPa were obtained with 40% MFC loading. In summary, this study showed that waste mango seed resource can be used to extract useful starch for use as a sustainable bio-derived resin to replace edible starch-based resins. Properties of MFC/MSS biocomposites were also comparable to some petroleum-based resins and can be used to replace them.

ACKNOWLEDGMENTS

The authors acknowledge and thank NSF-CREST (Grant 1137681) and Wallace Foundation for partially funding this work. The authors also would like to acknowledge the use of Cornell Center for Materials Research (CCMR) facilities supported by NSF (award no. DMR-1120296).

REFERENCES

1. Thakur, M. K.; Thakur, V. K.; Prashant, R. *Nanocellulose Polymer Nanocomposites: Fundamentals and Applications*, 1st ed.; John Wiley & Sons: Salem, Massachusetts, **2014**; p 1.
2. Netravali, A. N.; Chabba, S. *Mater. Today* **2003**, *6*, 22.
3. Ghosh Dastidar, T.; Netravali, A. N. *Green Chem* **2013**, *15*, 3243.
4. Das, K.; Ray, D.; Bandyopadhyay, N.; Gupta, A.; Sengupta, S.; Sahoo, S.; Mohanty, A.; Misra, M. *Ind. Eng. Chem. Res.* **2010**, *49*, 2176.

5. Ghosh Dastidar, T.; Netravali, A. N. *Carbohydr. Polym.* **2012**, *90*, 1620.
6. Lodha, P.; Netravali, A. N. *J. Mater. Sci.* **2002**, *37*, 3657.
7. Huang, X.; Netravali, A. *Compos. Sci. Technol.* **2007**, *67*, 2005.
8. Chang, P. R.; Jian, R.; Yu, J.; Ma, X. *Carbohydr. Polym.* **2010**, *80*, 420.
9. Dufresne, A. *Monomers, Polymers and Composites From Renewable Resources*, 1st ed.; Elsevier: Oxford, UK, **2008**; p 401.
10. Guan, J.; Eskridge, K. M.; Hanna, M. A. *Ind. Crop. Prod.* **2005**, *22*, 109.
11. Ghosh Dastidar, T.; Netravali, A. N. *J. Biobased Mater. Bio.* **2012**, *6*, 1.
12. Kalambur, S.; Rizvi, S. S. *J. Plast. Film Sheet* **2006**, *22*, 39.
13. Kazmi, A.; Shuttleworth, P. *The Economic Utilisation of Food Co-products*, 1st ed.; The Royal Society of Chemistry: Cambridge, UK, **2013**; p 64.
14. Rahman, M. M.; Ho, K.; Netravali, A. N. *J. Appl. Polym. Sci.* **2015**, *132*, DOI: 10.1002/app.41291.
15. Rahman, M. M.; Netravali, A. N. *ACS Sustain. Chem. Eng.* **2014**, *2*, 2318.
16. Kaur, M.; Singh, N.; Sandhu, K. S.; Guraya, H. S. *Food Chem.* **2004**, *85*, 131.
17. Kittiphoom, S.; Sutasinee, S. *Int. Food Res. J.* **2013**, *20*, 1145.
18. Solís-Fuentes, J.; Durán-de-Bazúa, M. *Bioresource Technol.* **2004**, *92*, 71.
19. Schieber, A.; Stintzing, F.; Carle, R. *Trends Food Sci. Tech.* **2001**, *12*, 401.
20. Tisserand, R.; Young, R. *Essential Oil Safety: A Guide for Health Care Professionals*, 2nd ed.; Churchill Livingstone Elsevier: **2013**; p 344.
21. Kapoor, V. *Nat. Prod. Rad.* **2005**, *4*, 306.
22. Nilani, P.; Raveesha, P.; Kasthuribai, N.; Duraisamy, B.; Dhamodaran, P.; Elango, K. *J. Pharm. Sci. Res.* **2010**, *2*, 178.
23. Abdalla, A. E.; Darwish, S. M.; Ayad, E. H.; El-Hamahmy, R. M. *Food Chem.* **2007**, *103*, 1134.
24. Khalil, H. A.; Bhat, A.; Yusra, A. I. *Carbohydr. Polym.* **2012**, *87*, 963.
25. Tanpichai, S.; Quero, F.; Nogi, M.; Yano, H.; Young, R. J.; Lindström, T.; Sampson, W. W.; Eichhorn, S. J. *Biomacromolecules* **2012**, *13*, 1340.
26. Patil, N. V.; Netravali, A. N. *ACS Sustain. Chem. Eng.* **2016**, *4*, 1756.
27. Ghosh Dastidar, T.; Netravali, A. *ACS Sustain. Chem. Eng.* **2013**, *1*, 1537.
28. Singh, N.; Singh, J.; Kaur, L.; Sodhi, N. S.; Gill, B. S. *Food Chem.* **2003**, *81*, 219.
29. Singh, J.; Singh, N. *Food Hydrocolloid.* **2003**, *17*, 63.
30. Krueger, B.; Knutson, C.; Inglett, G.; Walker, C. *J. Food Sci.* **1987**, *52*, 715.
31. Biliaderis, C.; Maurice, T.; Vose, J. *J. Food Sci.* **1980**, *45*, 1669.
32. Lee, E. S.; Kim, H. J. *J. Appl. Polym. Sci.* **2001**, *81*, 654.
33. Reddy, N.; Yang, Y. *Food Chem.* **2010**, *118*, 702.
34. Cantero, G.; Arbelaiz, A.; Llano-Ponte, R.; Mondragon, I. *Compos. Sci. Technol.* **2003**, *63*, 1247.
35. Brahmakumar, M.; Pavithran, C.; Pillai, R. *Compos. Sci. Technol.* **2005**, *65*, 563.
36. Netravali, A.; Henstenburg, R.; Phoenix, S.; Schwartz, P. *Polym. Compos.* **1989**, *10*, 226.
37. Qiu, K.; Netravali, A. N. *Compos. Sci. Technol.* **2012**, *72*, 1588.
38. Cheng, Q.; Wang, S.; Rials, T. G.; Lee, S. H. *Cellulose* **2007**, *14*, 593.
39. Huang, X.; Netravali, A. *Compos. Sci. Technol.* **2009**, *69*, 1009.
40. Felix, J. M.; Gatenholm, P. *J. Appl. Polym. Sci.* **1991**, *42*, 609.
41. Zhang, S. D.; Zhang, Y. R.; Huang, H. X.; Yan, B. Y.; Zhang, X.; Tang, Y. *J. Polym. Res.* **2010**, *17*, 43.
42. Tingaut, P.; Zimmermann, T.; Lopez-Suevos, F. *Biomacromolecules* **2009**, *11*, 454.